Network growth under the constraint of synchronization stability

Chenbo Fu[1,2] and Xingang Wang[1,2,*]

[1]*Institute for Fusion Theory and Simulation, Zhejiang University, Hangzhou 310027, China*

[2]*Department of Physics, Zhejiang University, Hangzhou 310027, China*

(Received 15 March 2011; revised manuscript received 3 May 2011; published 2 June 2011)

While it is well recognized that realistic networks are typically growing with time, the dynamical features of their growing processes remain to be explored. In the present paper, incorporating the requirement of synchronization stability into the conventional models of network growth, we will investigate how the growing process of a complex network is influenced by, and also will influence, the network collective dynamics. Our study shows that, constrained by the synchronization stability, the network will be growing in a *selective and dynamical* fashion. In particular, we find that the chance for a new node to be accepted by the growing network could have a large variation, i.e., it follows roughly a power-law distribution. Furthermore, we find that, with the dynamical growth, the network is always developed into structures of clear scale-free features, despite the form of the link attachment (preferential or random). The dynamical properties of network growth are studied using the method of eigenvalue analysis, and they are verified by direct simulations of coupled chaotic oscillators. Our study implies that, driven by the network collective dynamics, network growth could also be highly dynamical.

DOI: 10.1103/PhysRevE.83.066101 PACS number(s): 89.75.Hc, 05.45.−a

I. INTRODUCTION

Complex networks have the feature of growth. This is evidenced by numerous real-world systems, man-made or natural, and has been commonly regarded as one of the key ingredients supporting the evolution of realistic networks [1–3]. In particular, in the pioneering work of Barabási and Albert (BA) [4], which takes into account the mechanisms of network growth and preferential link attachment, a growth network model capable of reproducing the power-law degree distribution observed in many realistic complex systems has been proposed. In the BA growth model, starting from a small nucleus of globally connected nodes, the size of the network is linearly increased by the subsequent addition of new nodes. This type of network growth, however, is quite different from the empirical observations of many realistic systems, where the network growth is often shown to be nonmonotonic and intermittent [5–9]. For example, in a technological network such as an electric power grid [10–12], the introduction of a new node (power station) will increase the load of the existing nodes, which, once overloaded, will be broken down and may trigger an avalanche over the network [13–15]. As a result, the network size no longer increases monotonically, but rather fluctuates with time. Even for situations in which the network size increases monotonically, it is often hard to claim that the growing process is smooth. Consider the evolution of an ecological system as an example [16,17]. When a new node (species) is introduced, depending on the stability of the enlarged system, this new node may either die off or overcome the competitions with the existing nodes and survive [17]. In this case, while new nodes are subsequently introduced to the system, only some of the additions are accepted, i.e., the size of the network grows in an intermittent fashion [18]. The nonmonotonic, intermittent features of network growth thus suggest that, driven by the collective dynamics of the network, the growing process of complex networks could also be highly *dynamical*—a point that has been largely overlooked in previous studies.

Dynamical growth raises new questions, as well as new challenges, in the study of evolutionary networks. For a realistic network, to keep up with the changing environment or to improve system performance, the network structure must be continuously modified or updated [3]. To cope with this situation in theory, different evolutionary network models have been proposed and investigated in the past [13–21]. Among these studies, a popular approach to modeling network evolution is to rewire the network links according to the network's collective dynamics, e.g., for instance, the rewiring of the network links based on the situation of node synchronization [22–26]. (For a description of the recent progress in this direction of research, please refer to Ref. [27] and references therein.) In this study, an important feature of network evolution is that the network size remains *fixed*. When the network size is changeable, such as in the growing network to be studied in the following, the evolution properties will be changed significantly. These changes are mainly reflected in two aspects: the manner and mechanism of the evolution. In a growing network, the introduction of a new node will only modify the local structure of the attached nodes while leaving the remaining structure of the network unchanged, e.g., the BA growth model [4]. In this way, the network structure is developed in an *accumulative* fashion. This feature of network evolution is different from that of the previous models of fixed-size networks. For instance, in the model of link rewiring, depending on the instant states of the nodes, a link may be rewired repeatedly during the process of network evolution [28–31]. Meanwhile, in terms of the evolution mechanism, in a growing network it is the coevolution between the *two dynamics*—one for the network growth and the other for the network collective dynamics (synchronization)—that guides the evolution direction, while for the case of a fixed-size network, it is the interplay between the network structure and collective dynamics that plays the key role [32–36]. For the

*Corresponding author: wangxg@zju.edu.cn

above new features of a growing network, it is intriguing to see what the coevolution is between the network growth and collective dynamics.

In the present paper, employing synchronization as the typical collective dynamics of a complex network [27,32], we will investigate how the growing process of a network could influence, and in turn be influenced by, the network synchronization. In particular, we will incorporate the requirement of global complete synchronization into the growth of a complex network of coupled nonlinear oscillators, and investigate how the two dynamics, the growing dynamics and the node dynamics, affect each other during the course of network evolution. Our main finding is that, constrained by synchronization stability, *the growing process of the network could be highly dynamical*. More specifically, we find that the time interval for a new node to be successively accepted by the growing network has a large variation, i.e., it roughly follows a power-law scaling. Furthermore, we also find that, with dynamical growth, the scale-free feature can naturally emerge in the network structure regardless of the form of the link attachment. These findings have the potential to extend our knowledge of evolutionary networks considerably, as they could bring new attention to the rich dynamics of network growth. Our work is partially stimulated by the recent study of Ref. [18], in which the *topological* properties of a growing network under the stability constraints of a stationary state are investigated. Contrary to Ref. [18], we focus here on the *dynamical* properties of the growing process, with special attention given to the coevolution between network growth and the network's collective dynamics.

The rest of the paper is organized as follows. In Sec. II, we will present our model of a growing dynamical network and introduce the method of eigenvalue analysis. In Sec. III, we will investigate in detail the growth of a constrained BA network. The dynamical features of the growing process will be described and characterized, as well as the topological properties of the generated network. In Sec. IV, we will study the growing process of the constrained random network (the new nodes are attached to the network in a random fashion), and the emergence of a scale-free feature during the process of network evolution will be highlighted and addressed. In Sec. V, based on the method of eigenvalue analysis, we will explore the underlying mechanisms of the observed dynamical growth, together with the influence of the synchronization constraint on the form of the link attachment. Finally, In Sec. VI we will give our discussions and conclusion.

II. THE MODEL

Our first model of growing network is adopted from the BA model [4], but with nonlinear dynamics on the network nodes. Specifically, starting from a small, synchronizable nucleus of m_0 nonlinear oscillators (nodes), at each time step δt_g of the network growth a new node will be introduced, which is connected to m of the existing nodes by the manner of preferential attachment $\Pi_i = k_i / \sum_j k_j$, with $i, j = 1,2,\ldots,n$ the node indices and k_i the degree of the ith node. If the addition of the new node does not break the stability of network synchronization, then the new node will be accepted and the network size will be increased by one; otherwise, the new node will be rejected and the network structure will remain unchanged. Here, for simplicity, we set the local dynamics of the nodes to be identical, and we employ the scheme of normalized coupling strength [35,36]. With these settings, the dynamics of the ith oscillator reads

$$\dot{\mathbf{x}}_i = \mathbf{F}(\mathbf{x}_i) + \frac{\varepsilon}{k_i} \sum_{j=1}^{n} a_{ij}[\mathbf{H}(\mathbf{x}_j) - \mathbf{H}(\mathbf{x}_i)], \tag{1}$$

where $\mathbf{F}$ and $\mathbf{H}$ represent the dynamics of the isolated oscillator and the coupling function, respectively. The network structure is characterized by the adjacency matrix $\{a_{ij}\}$, in which $a_{ij} = 1$ if oscillators i and j are directly connected, and $a_{ij} = 0$ otherwise. $\varepsilon > 0$ is the uniform coupling strength, which is also the total incoming coupling strength of each oscillator, i.e., the node coupling intensity. Please note that the coupling strength that i receives from j, $c_{ij} = (\varepsilon a_{ij})/k_i$, in general is different from the one that j receives from i, i.e., the network is weighted and directed.

Due to the feature of network growth, in Eq. (1) the network size is no longer fixed, but rather it is *timely varying*, i.e., $n \sim n(t)$. This raises the problem of time-scale separation in characterizing the network evolution [18,37], which has a direct influence on the synchronization constraint. Let T_s and T_g be the time scales that characterize the network synchronization and growth, respectively. (In a practical situation, T_s could be the transient time for network synchronization and T_g could be the time interval between two adjacent node additions.) If $T_s \gg T_g$, due to the "slow" response of the network's collective dynamics, the synchronization constraint will have no impact on network growth, and the network evolution will be identical to that of the BA model. In contrast, if $T_s \ll T_g$, the synchronization dynamics is much faster than the growth dynamics, in which case the growing process can be regarded as adiabatic. For the latter case, the network synchronization will play its role and influence the network growth. As a result, the generated network will be different from that of the BA model. For both cases, the time scales of the two dynamics (synchronization and growth) can be well separated, and the network size is increased monotonically during the course of network evolution. The situation will be much more complicated when the two time scales are comparable, e.g., $T_s \sim T_g$ [37]. In that case, the two dynamics are fully coupled and, depending on the instant network structure and collective dynamics, the network size may either increase or decrease, i.e., the growth is nonmonotonic. For the sake of simplicity, in the present work we will concentrate on only the case of $T_s \ll T_g$, which is generally the situation in technological and neural networks, e.g., for example, the plasticity of neuron synapses [38].

Having separated the time scales, we are now able to decouple the dynamics of network synchronization from that of network growth in addition to characterizing the network synchronizability by the network topology. This is done using the method of the master stability function (MSF) [39–41], with the following details. Assuming that at moment t_g the network has $n-1$ synchronized oscillators and a new oscillator is introduced, then whether the enlarged network (of

size n) is still synchronizable is determined by the following set of variational equations:

$$\dot{\delta \mathbf{x}_i} = \mathbf{DF}(\mathbf{x}_s) + \frac{\varepsilon}{k_i} \sum_{j=1}^{n} a_{ij} \mathbf{DH}(\mathbf{x}_s)[\delta \mathbf{x}_j - \delta \mathbf{x}_i], \qquad (2)$$

with $i = 1,2,\ldots,n$ the node index. In Eq. (2), $\mathbf{x}_s$ is the synchronous manifold to which all the oscillators are assumed to be synchronized, $\delta \mathbf{x}_i = \mathbf{x}_i - \mathbf{x}_s$ is the trajectory divergence of the ith oscillator from $\mathbf{x}_s$, and $\mathbf{DF}(\mathbf{x_s})$ and $\mathbf{DH}(\mathbf{x_s})$ are the Jacobian matrices of the corresponding vector functions evaluated on $\mathbf{x}_s$. To keep the network synchronizable, a necessary condition is that all the trajectory divergences $\{\delta \mathbf{x}_i\}$ are damping with time. Projecting $\{\delta \mathbf{x}_i\}$ into the eigenspace spanned by the eigenvectors $\{\mathbf{v}_i\}$ of the coupling matrix $C = \{a_{ij}/k_i\}$, the variational equations of Eq. (2) can be diagonalized into n decoupled eigenmodes in the block form

$$\dot{\mathbf{y}}_l = [\mathbf{DF}(\mathbf{x}_s) + \varepsilon \lambda_l \mathbf{DH}(\mathbf{x}_s)]\, \mathbf{y}_l, \quad l = 1, \ldots, n, \qquad (3)$$

where $\mathbf{y}_l$ is the lth eigenmode transverse to the synchronous manifold $\mathbf{x}_s$, and $0 = \lambda_1 \geqslant \lambda_2 \geqslant \cdots \geqslant \lambda_n$ are the eigenvalues of the coupling matrix C. Among the n eigenmodes, the one associated with $\lambda = 0$ represents the motion parallel to the synchronous manifold, and network synchronization is achievable only when all other eigenmodes, $\mathbf{y}_j, j = 1, \ldots, n$, are damping with time, i.e., the largest Lyapunov exponent of each eigenmode is negative, $\Lambda(\varepsilon \lambda_j) < 0$. For typical nonlinear systems, it has been shown that the value of $\Lambda(\sigma)$ is negative only in a bounded range in the parameter space, $\sigma \in (\sigma_1, \sigma_2)$ [42]. Thus, to make the synchronous state stable, the sufficient condition is that all the values of $\sigma_j = \varepsilon \lambda_j$ should be contained in the range (σ_1, σ_2). In particular, we should have $\varepsilon \lambda_2 < \sigma_2$ and $\varepsilon \lambda_n > \sigma_1$ simultaneously, which leads to the following necessary condition for network synchronization: $R = \lambda_n/\lambda_2 < \sigma_1/\sigma_2 = R_c$. For a network of undefined node dynamics, e.g., one in which the values of σ_1 and σ_2 exist but are not given, generally the smaller the eigenratio R is, the higher the probability is that the network could be synchronized. In this regard, another way to characterize the network synchronizability is simply to calculate the eigenratio R, which is dependent on only the network coupling matrix C.

With the assumption of time-scale separation and using the MSF method, our model of synchronization-constrained network growth can now be described as follows. With a predefined eigenratio R_c, which is determined by the dynamics of the isolated oscillator, at each time step of the network growth we introduce a new oscillator into the system and calculate the eigenratio R of the enlarged network. If $R < R_c$, then we say that the enlarged network is synchronizable and the new oscillator will be accepted; otherwise, the enlarged network is regarded as nonsynchronizable and the new oscillator will be rejected. The main task of the present work is merely to explore the dynamical properties of the network-growing process, as well as its consequences to the network structure.

III. THE GROWTH OF CONSTRAINED BA NETWORK

Before presenting our numerical results, we would like first to give a qualitative description of the possible influence of synchronization stability on network growth based on the method of eigenvalue analysis discussed above. This will be helpful in our selection of the network parameters in the following simulations, as well as giving an intuitive understanding of the mechanism of network evolution. Since we are interested in the case of a bounded MSF, to judge whether the growing network is synchronizable, we only need to check the behaviors of λ_2 and λ_n, i.e., the two boundary eigenvalues of the network coupling matrix. Without the requirement of synchronization stability (or in the case of $R_c \gg R$), the boundary eigenvalues will be of smooth trajectories. As schematically plotted in Fig. 1, with the increase of the network size n, the value of λ_2 will be gradually increased from $-n/(n-1)$ (the case for a globally connected network) to the limit $\tilde{\lambda}_2 \approx 2/\sqrt{\langle k \rangle} - 1$; in the meantime, λ_n will be decreased from $-n/(n-1)$ to $\tilde{\lambda}_n \approx -2/\sqrt{\langle k \rangle} - 1$. Here, $\langle k \rangle = 2m$ is the average network degree, and $\tilde{\lambda}_{2,n}$ are the theoretical predications obtained for large-scale complex networks [43,44].

When synchronization stability is required, through the critical eigenratio R_c, the node dynamics will influence the behaviors of λ_2 and λ_n. More specifically, the critical eigenratio will set two new limits, $\lambda_{2,n}^c$, for the developments of λ_2 and λ_2. During the process of network growth, once $\lambda_{2,n}$ touch these new limits, they will be "stopped" immediately and stay around there afterward. So, to make the synchronization constraint have an effect, the necessary condition is $\lambda_2^c < \tilde{\lambda}_2$ or $\lambda_n^c > \tilde{\lambda}_n$, i.e., the value of R_c should be small enough. It should be noted that, even for a small value of R_c, the synchronization constraint does not have an effect until the network size exceeds some critical value, n_c. Here, n_c is defined as the point at which $R(n) = R_c$, which denotes the activation of the synchronization constraint. As schematically plotted in Fig. 1, in the region of $n < n_c$, the behaviors of λ_2 and λ_n are identical to that in the nonconstrained case, indicating a free growth of the network, while for $n > n_c$, the values of $\lambda_{2,n}$ remain around the new limits $\tilde{\lambda}_{2,n}$. Thus, in the region of $n > n_c$, to keep the network growing, the new node should be carefully selected. Speaking alternatively, in this region there is a chance for the new node to be accepted by the growing network. At this point, we are interested in the following questions: (i) What is the probability for the new node to be accepted? (ii) When will the new node be successfully accepted? (iii) What will the structure of the generated network look like?

Guided by the schematic plot of Fig. 1, we set the parameters in our model of the constrained BA network as $m_0 = 10$, $m = 4$, and $R_c = 4$. The growing process is stopped when the network has a size $n = 2 \times 10^3$. We begin by checking the behaviors of the boundary eigenvalues, $\lambda_{2,n}$, to figure out the critical network size, n_c. In Fig. 2, we plot the variations of $\lambda_{2,n}$ as a function of the network size for both the constrained and nonconstrained networks (the standard BA model). As expected, it is seen that the two sets of eigenvalues are identical when $n < 129$, but they diverge from each other when $n > 129$. From this observation,

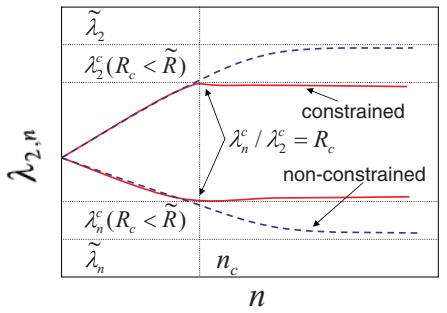

FIG. 1. (Color online) A schematic plot showing the possible influence of the synchronization constraint on the behaviors of the boundary eigenvalues, $\lambda_{2,n}$. Without the synchronization constraint, $\lambda_{2,n}$ approach the theoretical limits $\tilde{\lambda}_{2,n}$ (the blue-dashed curves). When the synchronization constraint is added ($R_c < \tilde{R}$), the behaviors of $\lambda_{2,n}$ change at a critical network size n_c, and stop at the new limits $\tilde{\lambda}_{2,n}^c$ set by the node dynamics (the red-solid curves).

we thus identify $n_c = 129$. A slight difference between the predication (Fig. 1) and the numerical results (Fig. 2) is that, instead of staying on some fixed values, here λ_2 and λ_n are found to be of small fluctuations after n_c. The fluctuations are understandable because in our model, the synchronization stability is characterized by the eigenratio $R = \lambda_n/\lambda_2$ instead of each individual eigenvalue.

We next investigate the dynamical properties of the growing process in the constrained network. Notice that a direct consequence of the synchronization constraint on network growth is the failure of some node additions, i.e., it may take many attempts for the network to adopt a new node. To explore the growing dynamics, the variation and distribution of the failed additions are thus the first things in which we are interested. With the same set of network parameters as in Fig. 1 ($m_0 = m = 4, R_c = 4$), we regrow the network, this time keeping a record of the failed additions. Denoting δn_g as

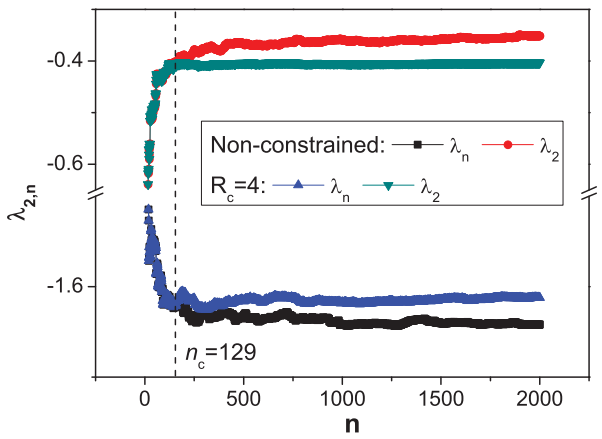

FIG. 2. (Color online) The variations of the boundary eigenvalues, $\lambda_{2,n}$, as a function of the network size for the nonconstrained and constrained network growths. The network parameters are $m_0 = 10$, $m = 4$, and the growing process is stopped at $n = 2 \times 10^3$. For the constrained case, the critical eigenratio is set as $R_c = 4$. The two sets of eigenvalues are differentiated at the point $n_c = 129$, indicating the activation of the synchronization constraint at this point in the constrained network.

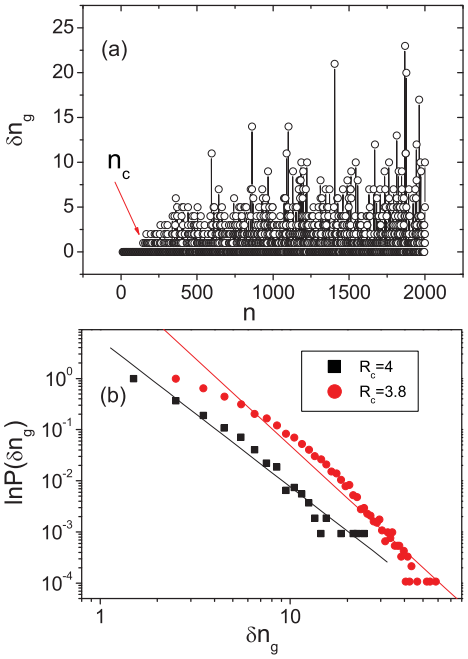

FIG. 3. (Color online) The intermittent growth of the constrained network. The network parameters are the same as those in Fig. 1. (a) For $R_c = 4$, the number of failed additions, δn_g, as a function of the network size. (b) The distributions of δn_g, which follow roughly a power-law scaling. For $R_c = 4$, the fitted exponent is about -2.87; for $R_c = 3.8$, it is about -3.4. The results of (b) are averaged over 24 network realizations.

the number of failed additions for the network to successfully adopt a new node, in Fig. 3(a)) we plot the variation of δn_g as a function of the network size. It is shown that, after the critical size n_c, the value of δn_g varies wildly in a wide range, $\delta n_g \in$. Since in our model the new nodes are introduced with a constant speed (with a time interval δt_g), the variation of δn_g thus manifests an *intermittent* growing of the network. To explore this intermittency in depth, we plot in Fig. 3(b) the distribution of δn_g. The distribution is found to follow a power-law scaling, with the fitted exponent about -2.87. It is noted that, with the change of the synchronization constraint (the value of R_c), both the range and the distribution of δn_g will be adjusted, as indicated by the results of $R_c = 3.8$ plotted in Fig. 3(b).

When will a node be successfully added? Or, speaking alternatively, which nodes in the existing network are more likely to accept the new node? This is the second question that we are interested, and it is an important step toward a full understanding of the network growing dynamics. To investigate, this time we record the degree information, k_f, of the nodes in the network that are attached by the new node but failed to accept it (degree information of the failed additions), and we make an analysis for the distribution. In our simulations, to generate a network of size $n = 2 \times 10^3$ under the constraint $R_c = 4$, there are a total of about 4×10^3 failed additions, which gives about 8×10^3 records on k_f. The distribution of k_f is plotted in Fig. 4(a). An interesting finding is that the distribution is composed of two well-separated scalings. Specifically, in the region of $k_f \in [4, 100]$ we have

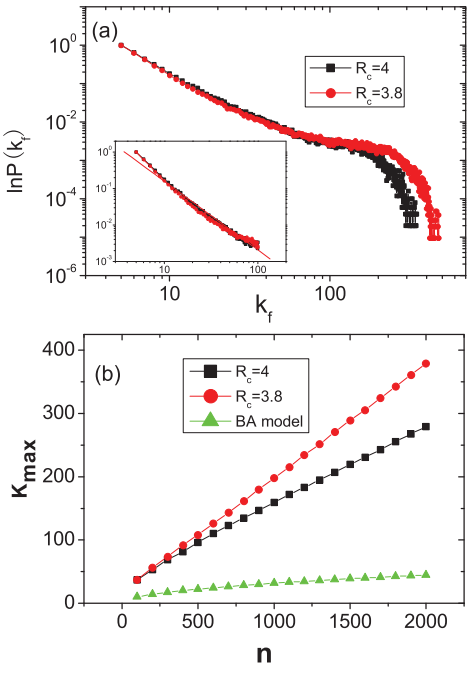

FIG. 4. (Color online) The network parameters are the same as those in Fig. 2. (a) The degree distribution, $P(k_f)$, of the nodes that failed to accept the new node during the process of network growth. The distribution is found to be composed of two separate scalings. For $k_f \in [4,100]$, it follows roughly a power-law scaling (inset), with the fitted exponent $\gamma' \approx -1.9$, while for $k_f > 100$, the distribution is roughly exponential, $P(k_f) \sim \exp(-1 \times 10^{-2} k_f)$. (b) Under different synchronization constraints, the increase of the largest node degree, $k_{\max}$, as a function of the network size. For the nonconstrained growth, we have $k_{\max} \propto n^{1/2}$; while for constrained growth, we have roughly $k_{\max} \propto n$. The results are averaged over 24 network realizations.

$P(k_f) \sim k_f^{\gamma'}$ with $\gamma' \approx -1.9$, while in the region $k_f > 100$ we have $P(k_f) \sim \exp(-1 \times 10^{-2} k_f)$. This feature of two-scaling distribution is general for the constrained network, as suggested by the results of $R_c = 3.8$ plotted in the same figure. An important finding that can be inferred from this distribution is that, comparing with the small-degree nodes, the large-degree nodes in the network are more likely to accept the new node. (A more detailed analysis will be given later.) This is especially the case for the behavior of the large-degree nodes in the network. As a matter of fact, in our simulations it is found that, at each time step of the network growth, the new node is always accepted if it is attached to the largest-degree node. This fashion of node attachment thus indicates the following: compared with the BA model, in a constrained network the largest degree, $k_{\max}$, increases more *rapidly*. This conjecture is well verified by simulations. In Fig. 4(b), we plot the variation of $k_{\max}$ as a function of n for different cases of network growth, where it is seen clearly that, for the constrained growth, $R_c = 4$ or 3.8, we have $k_{\max} \propto n$, while for the nonconstrained growth (the BA model), we have $k_{\max} \propto n^{1/2}$ [45].

The special form of the distribution $P(k_f)$ plotted in Fig. 4(a) implies a new type of link attachment (different from preferential attachment) caused by the synchronization constraint. The reasoning is the following. During the process of network growth, if the new node is rejected with equal probability, i.e., without considering the degree of the attached nodes, then the network will be still growing by the mechanism of preferential attachment, $\Pi \sim k$, and, as a sequence, the network will still possess the power-law degree distribution, $P(k) \sim k^{-\gamma}$, with $\gamma \approx 3$ [4]. If this is the case, then we will have $P(k_f) \sim P(k)\Pi(k) \sim k^{-2}$ for the degree of the failed nodes. Apparently, this is not the case observed in numerical simulations, where $P(k_f)$ is found to have an exponential tail for large values of k_f [Fig. 4(a)]. That is, the real attaching probability of the constrained network deviates from the preferential attachment. As preferential attachment plays a key role in generating a scale-free network, we are thus interested in the structure of the constrained network. In particular, we want to compare it with the nonconstrained BA network and determine the difference.

In our study, the structure of the constrained network is characterized by the following three quantities [1]: the degree distribution $P(k)$, the average diameter $\langle d \rangle$, and the average clustering coefficient $\langle c \rangle$. The degree distributions of both the constrained and nonconstrained networks are plotted in Fig. 5(a), which is obtained from networks of size $n = 2 \times 10^3$. It is seen that, despite the value of R_c, in the constrained networks the scale-free feature still persists in a wide range of degree. Specifically, in the region of $k \in [4,100]$, we have $P(k) \sim k^{-2.8}$ for both the cases of $R_c = 4$ and 3.8, which is almost identical to that of the nonconstrained case. However, in the region of large degree, $k > 100$, the constrained network has a clearly long tail. As shown in Fig. 5(a), for the nonconstrained network the largest degree is 172, while for $R_c = 4$ and 3.8 the largest degree is 293 and 428, respectively. Based on this observation, the constrained network might be regarded as the embedding of a few super-degree nodes in the conventional BA-type scale-free network.

Combining the results of Figs. 4(a) and 5(a), we get the following features of the dynamical growth in a constrained network. When the new node is not attached to the large-degree nodes in the network, it has an *equal chance* to be rejected, regardless of the degree of the attached nodes. (The definition of large degree is dependent on the network parameters. For a network of $m = 4$ and $n = 2 \times 10^2$, we regard $k > 100$ as large.) This feature of equal rejection is drawn from the relationship between the two scalings, $P(k_f)$ and $P(k)$, that are obtained by numerical simulations. Statistically, the probability for a node of degree k to reject the new node is proportional to $P(k)\Pi(k)/P'(k)$, which, according to our numerical results, is almost constant ($\sim k^{0.1}$), i.e., an equal rejection. However, the rejecting probability is significantly reduced for the large-degree nodes, as can be partially seen from the exponential tail in the distribution of k_f [Fig. 4(a)]. Noticing the fact that such a tail is absent in the distribution $P(k)$, the quick decrease of $P(k_f)$ thus also implies a significant *variation* of the rejecting probability among the large-degree nodes. As a consequence, in the constrained network the largest degree, $k_{\max}$, is expected to increase rapidly with the network size, a fact shown in Fig. 4(b).

It is worth noticing that the special form of degree distribution found in the constrained network, i.e., power-law scaling followed by a long tail, is also observed in many

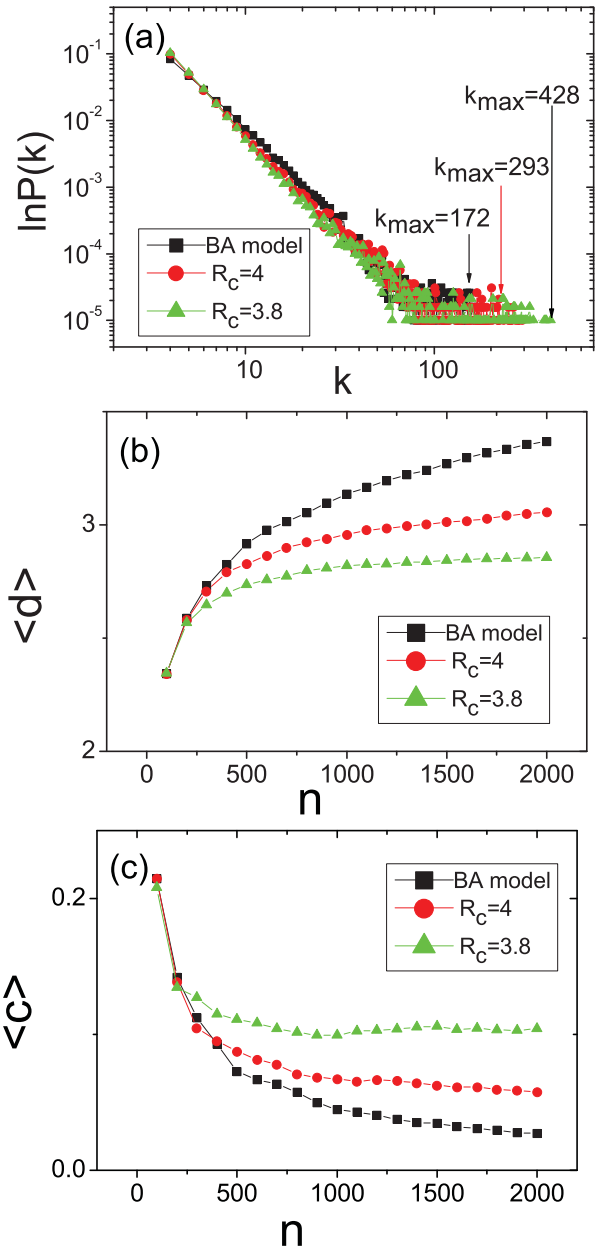

FIG. 5. (Color online) The topological properties of the constrained networks generated by $R_c = 4$ and 3.8. The other network parameters are the same as those in Fig. 2. (a) The degree distributions of the constrained networks. The fitted slope is about -2.8 in the region of $k \in [4,100]$. With the decrease of R_c, the distribution is found to be gradually extended to the region of large degree. Each datum is averaged over 24 network realizations. (b) The variation of the network average diameter $\langle d \rangle$ with the network size. (c) The variation of the network average clustering coefficient $\langle d \rangle$ with the network size. As a comparison, the results of the nonconstrained BA scale-free network are also plotted in each subgraph.

realistic systems, and might have important implications on system performance [2]. For instance, in studying the degree distribution of the Internet at the AS level [46], it is observed that the degree of a few of the network nodes is apparently larger than those predicted according to the BA model. For a technological network like the Internet, the embedding of a few super-degree nodes could largely improve the system performance, as the average network diameter can be significantly reduced. However, with the emergence of super-degree nodes, the risk of network security will also be increased. For instance, the network connectivity could be affected significantly if the few super-nodes are intentionally removed [47]. Thus, the sparse super-degree nodes embedded in realistic networks might be due to the balance between network performance and security.

The variations of the network average diameter, $\langle d \rangle$, and the average clustering coefficient, $\langle c \rangle$, with the network size are plotted in Figs. 5(b) and 5(c), respectively. (Please refer to Ref. [48] for detailed definitions of $\langle d \rangle$ and $\langle c \rangle$.) In Fig. 5(b), it is seen that, when the network size exceeds n_c, the value of $\langle d \rangle$ for the constrained network becomes smaller than that of the nonconstrained network. Moreover, with the increase of n, the difference between the constrained and nonconstrained networks is gradually enlarged. Also, by decreasing R_c, it is found that the curve of $\langle d \rangle$ is moving downward (the case of $R_c = 3.8$ in the figure). Similar behavior is also observed for the network clustering coefficient $\langle c \rangle$. As shown in Fig. 5(c), the curve of $\langle c \rangle$ for $R_c = 4$ is above that of the nonconstrained network, and is moving upward with the decrease of R_c. The decreased $\langle d \rangle$ (increased $\langle c \rangle$) in the constrained network is surely due to the emergence of the super-degree nodes. For the other network parameter fixed, in general the more heterogeneous the degree distribution is, the smaller (larger) is the average diameter (clustering coefficient) [48].

IV. THE CONSTRAINED NETWORK GROWTH UNDER RANDOM ATTACHMENT

As discussed in Ref. [1], both growth and preferential attachment are necessary to generate networks of scale-free property. For a growing network without preferential attachment, the generated network will be non-scale-free. For instance, if the new nodes are connected to the existing nodes in a random fashion, the generated network will have an exponential degree distribution [4,45], i.e., the random growth network. However, for some realistic networks where the preferential attachment is not satisfied naturally, the network structure is still observed to possess the scale-free feature, e.g., the cellular [49] and ecological networks [50]. This phenomenon has inspired studies about the alternative mechanisms of preferential attachment in network generation, e.g., the copying mechanism and edge redirection [51,52]. Here, inspired by the numerical findings that the link attachment can be modified by the synchronization constraint [Fig. 4(a)], we are curious to see what happens to the structure of the random growth network if it is constrained by the synchronization stability.

To check it out, in our second model the preferential attachment is replaced by a random attachment, while the other settings are the same as that of the constrained BA model investigated in the previous section. Still, we are interested in the dynamical features of the growth and the topological properties of the generated network. The distribution of the failed additions, δn_g, is plotted in Fig. 6(a), where the nonsmooth and intermittent features are observed again. Compared with the constrained BA model [Fig. 3(b)], it is

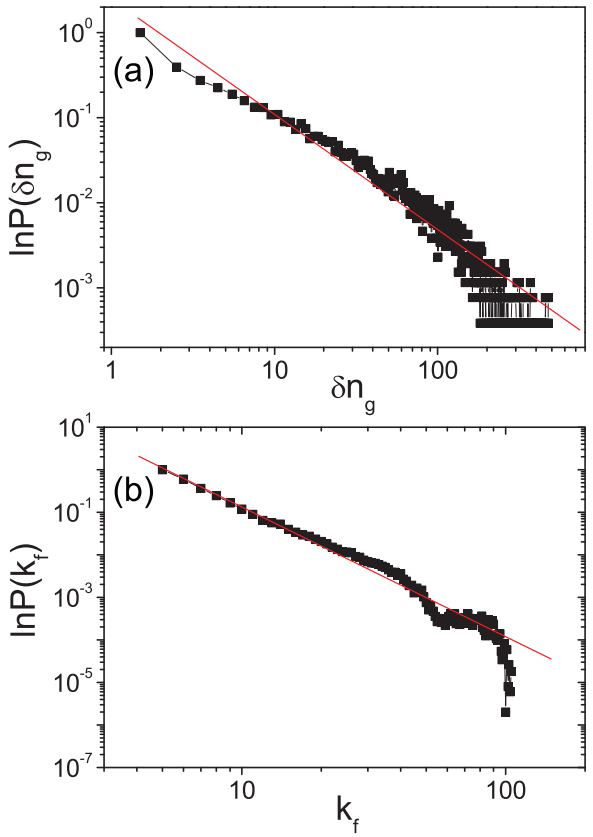

FIG. 6. (Color online) With a random attachment, the dynamical network growth under the constraint $R_c = 4$ is shown. The network parameters are the same as those in Fig. 2, but the growing process is stopped at $n = 600$. (a) The distributions of the failed additions δn_g, which roughly have a power-law distribution with a fitted exponent, is about -1.6. (b) The degree distribution of the attached nodes failed to accept the new nodes, which has a power-law scaling, with the fitted exponent about -3.4. The results are averaged over 24 network realizations.

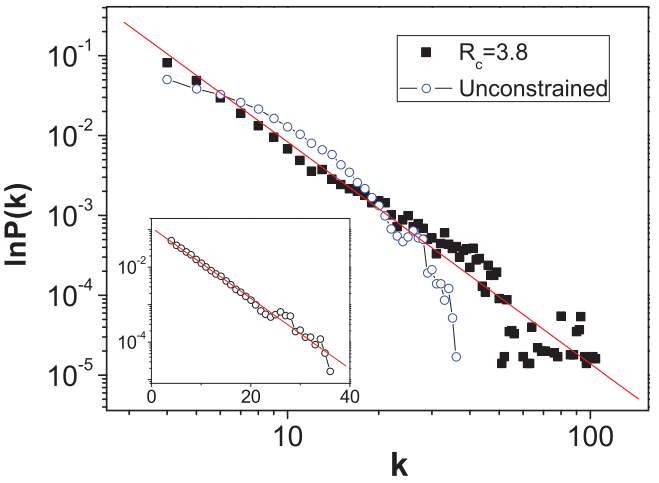

FIG. 7. (Color online) For $R_c = 4$, the degree distribution of the constrained random network of size $n = 600$ is shown. The distribution has the power-law scaling $P(k) \sim k^{-\gamma}$, with $\gamma \approx -2.7$. As a comparison, the degree distribution of the nonconstrained random network of the same size is also plotted, which has exponential scaling (inset). Each datum is averaged over 24 network realizations.

noticed that in Fig. 6(a) the value of δn_g varies in a much wider range (extended by about one order of magnitude) and has a more heterogeneous distribution (the fitted exponent is about -1.6, while in the constrained BA model it is about -3.4). The wild variation of δn_g implies that, compared to the constrained BA model, the growth of the constrained random network is much slower. In fact, in our simulations, with the same amount of trying additions (about 1×10^4), while the constrained BA network is grown to $n = 2 \times 10^3$, the size of the constrained random network is only about 600.

We next check the property of the failed additions in the constrained random network, i.e., the degree distribution, $P(k_f)$, of the nodes that failed to accept the new nodes during the process of network growth. The numerical results are plotted in Fig. 6(b). In contrast with the two-scaling distribution observed in the case of the nonconstrained BA network [Fig. 4(a)], it is seen that in the case of the constrained random network, the distribution is well fitted by a single power-law scaling, $P(k_f) \approx k_f^{\gamma'}$, with $\gamma' \approx -3.4$ [Fig. 6(a)]. As in this model the new node is originally attached to the network in a random fashion, it is somewhat surprising to see that here $P(k_f)$ shows a power-law scaling. Since the distribution $P(k_f)$ is also dependent on the degree distribution of the generated network, to explore the nature of the failed additions in depth, it is necessary to analyze the structure of the generated network.

The degree distribution of the constrained random network is plotted in Fig. 7. A novel finding is that, although it is of random attachment, the network has a clear scale-free feature. Specifically, we have $P(k) \sim k^{-\gamma}$, with the fitted exponent $\gamma \approx -2.7$. Compared with the case of the constrained BA network [Fig. 5(a)], it is also seen in Fig. 7 that the super-degree nodes disappear. To identify the scale-free feature of the generated network, we regenerate the network without the synchronization constraint and compare its degree distribution with that of the constrained case. As shown in the inset of Fig. 7, the degree distribution of the nonconstrained network follows the exponential scaling, which is clearly different from the constrained network.

How could a scale-free network be generated without preferential attachment? The key to answering this question is the synchronization constraint. Due to the constraint, only nodes that maintain synchronization stability are accepted during the process of network growth. Regarding node selection as a new mechanism of link attachment, the scale-free feature that appeared in the constrained random network thus seems to suggest the following: *the synchronization constraint plays a similar role to the preferential attachment in the network growth*. To verify this conjecture, a detailed study on the behavior of the eigenvalues of the growing network will be necessary, since it is the connection between the network structure (the eigenspectrum) and the the synchronization behaviors (the eigenratio). In particular, when a new node is introduced into the network, we need to calculate the new eigenvalue, λ_{new}, accompanying this new addition and evaluate its influence on the synchronization of the enlarged network.

V. MECHANISM ANALYSIS AND NUMERICAL VERIFICATIONS

A. Eigenvalue analysis

As we discussed in Sec. II, for the general case of a bounded MSF function, the network synchronizability is jointly determined by the smallest nonzero eigenvalue, λ_2, and the largest eigenvalue λ_n of the network coupling matrix. This means that if the addition of the new node does not change the values of λ_2 and λ_n of the network, then the network synchronizability will not be affected. Speaking alternatively, if at a moment the network contains n synchronizable nodes and a new node is introduced, it is highly possible that the new node will be accepted if the new eigenvalue, λ_{new}, is within the range $[\lambda_2,\lambda_n]$. It should be noted that in a networked system, the addition of a new node will also influence some of the existing eigenvalues, i.e., the eigenvalues are interdependent. However, for the influenced eigenvalues, a general feature is that they are close to λ_{new} in the eigenvalue spectrum [43]. Regarding this feature, the location of λ_{new} in the spectrum is thus of crucial importance to the stability of network synchronization. Specifically, the farther away λ_{new} is from the boundary eigenvalues in the existing eigenspectrum, the less the boundary eigenvalues will be affected, and the higher is the possibility that the new node will be accepted. Therefore, due to the synchronization constraint, the new eigenvalue (accompanied with the new node) is actually "preferentially" selected.

The "preferential" selection of the new eigenvalue is verified by numerical simulations. In Fig. 8 we plot the eigenspectrum of the growing network at different sizes, where it is clearly seen that the number of eigenvalues in the middle part of the spectrum increases much more quickly than that of the boundary regions. In particular, as the network size increases from $n = 500$ to 2×10^3, more than 30% of the new eigenvalues are found to be located in the narrow range of [0.9,1.1], while in the boundaries regions, with the same scope, it is less than 3%.

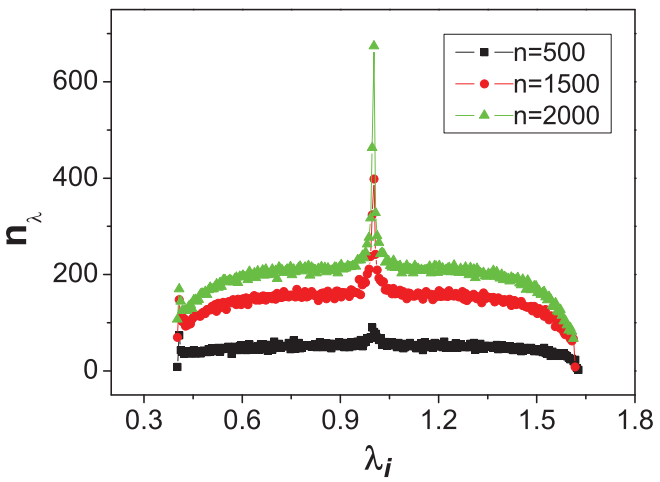

FIG. 8. (Color online) The evolution of the eigenspectrum in the model of a constrained random network with $R_c = 4$. A clear feature is that the middle part of the spectrum increases much more quickly than the boundary regions, indicating a "preferential" selection of the new eigenvalues due to the synchronization constraint.

B. Analysis of the star-structure network

How is the "preferential" selection of the new eigenvalue reflected in the node attachment? Because of the complicated relationship between the network nodes and eigenvalues (a many-to-many mapping) [53], in complex networks it is generally difficult to have a precise prediction of the relationship between the new eigenvalue and the attaching fashion of the new node. More specifically, to generate a predefined eigenvalue λ_{new}, we do not know how the new node should be attached to the network. Here, to investigate this question in a qualitative manner, we adopt in the following the simplified model of a star-structure network, which captures many essential features of the complex network. The star network considered here consists of $n-1$ nodes and $n-2$ links, with the node labeled 1 at the center and the other $n-2$ nodes at the periphery. Using the coupling scheme of Eq. (2), the star network has three distinct eigenvalues: $\lambda_1 = 0$, $\lambda_{i=2,\ldots,n-2} = -1$, and $\lambda_{n-1} = -2$. To study the correspondence between the attachment and the eigenvalue, we add a new node into this network by randomly attaching it with one of the existing nodes and monitoring the change of the eigenspectrum for the new eigenvalue. Due to the symmetry of the network structure, the enlarged network (of size n) has only two possibilities: the node is connected to either (i) the central node or (ii) one of the peripheral nodes.

For the first case, it is straightforward to see that the new addition brings in $\lambda_{\text{new}} = -1$, while all the "old" $n-1$ eigenvalues are kept unchanged. Since for the star network $\lambda \in [-2,0]$, the new eigenvalue is thus located in the middle of the eigenspectrum. For the second case, we have $n-4$ eigenvalues equal to -1, while the other eigenvalues are governed by the equation

$$2(n-2)(1+\lambda)^4 - (3n-7)(1+\lambda)^2 + (n-3) = 0. \quad (4)$$

From this equation, we get the following two new eigenvalues in the spectrum:

$$\lambda_2 = -1 + \sqrt{(n-3)/(2n-4)},$$
$$\lambda_{n-1} = -1 - \sqrt{(n-3)/(2n-4)}. \quad (5)$$

Clearly, $\lambda_2 > -1$ and $\lambda_{n-1} < -1$, i.e., the two new eigenvalues are away from the center of the eigenspectrum. Moreover, it can be seen from Eq. (5) that, with the increase of n, λ_2 and λ_{n-1} will approach the limits $-1 + 1/\sqrt{2}$ and $-1 - 1/\sqrt{2}$, respectively, i.e., toward the boundaries of the eigenspectrum. So, for this simplified network model, the correspondence between the new eigenvalue and the node attachment is clear: to add an eigenvalue at the middle part of the eigen-spectrum, we should attach "preferentially" the new node to the hub node; otherwise, to make the new eigenvalue appear in the boundary regions, the new node should be attached to the peripheral nodes.

Regarding the hub and peripheral nodes in the star network as special examples of the large- and small-degree nodes in the complex network, respectively, it is reasonable to expect that a similar correspondence (between the new eigenvalue and the node attachment) should be observed in our model of

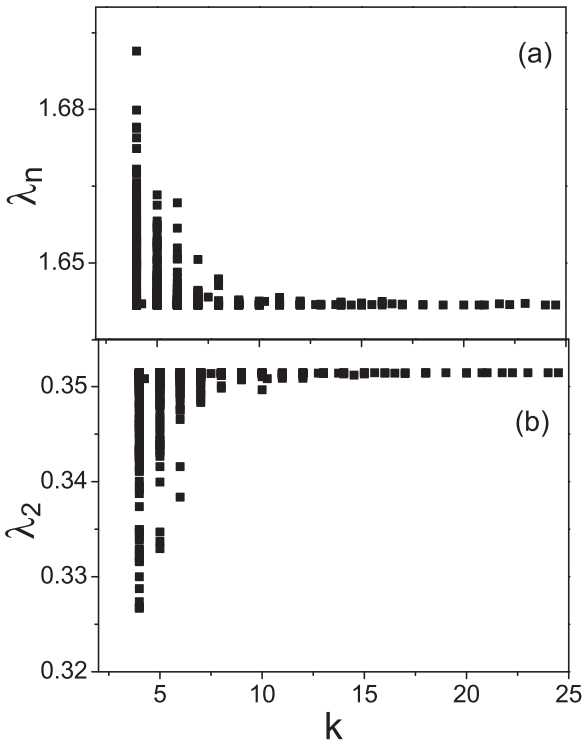

FIG. 9. For a standard BA network of size $n = 2 \times 10^3$ and average degree 8, the fluctuations of the boundary eigenvalues, λ_2 and λ_n, are shown when different nodes in the network are attached. As the degree of the attached node increases, the fluctuations are found to be gradually narrowed, implying that the network synchronizability is less affected by the node attached to the large-degree nodes.

a constrained network. To verify this, we generate a network of size $n = 2 \times 10^3$ (by the standard BA model), and randomly add a new node onto it. Here, for simplicity, the new node is set to have only one link. The addition is tried 500 times. For each addition, we record the degree, k, of the attached node in the network, and also the boundary eigenvalues, λ_2 and λ_n, of the enlarged network. The distribution of λ_2 and λ_n as a function of k is plotted in Fig. 9. It is seen that, as the degree of the attached node increases, the fluctuations of the boundary eigenvalues are gradually narrowed. That is, the larger the degree of the attached node is, the less variation there will be in the boundary eigenvalues—an indication of the link preferential attachment.

Now the emergence of scale-free feature in constrained random network (Fig. 7) can be explained heuristically as follows. The synchronization requirement poses a constraint on the behaviors of the boundary eigenvalues, $R = \lambda_n/\lambda_2 < R_c$, which, during the process of network growth, will guide the selection of the newly added eigenvalues. In particular, when a new eigenvalue is introduced, it is required that the boundary eigenvalues remain stable and are not influenced. This requirement makes it favorable to select the new eigenvalue from the intermediate regime of the eigenspectrum, while, to generate an intermediate eigenvalue, the new node will tend to connect to the large-degree nodes in the network. So, we see that in the constrained random network it is actually the synchronization constraint that provides the mechanism for preferential attachment. The logic behind the analysis is as follows: network synchronizability → eigenvalue selection → link preferential attachment.

C. Numerical verification

Let us now discuss the realistic situation. So far, all our findings are based on the method of eigenvalue analysis, in which many of the intrinsic properties of the node dynamics have been neglected. As we explained in the Introduction, the eigenvalue analysis is based on the assumption of time-scale separation, $T_s \ll T_g$, which, in a realistic situation, is usually not met. This is especially the case for large-scale networks, where the transient time for network synchronization could be very long [54,55]. In this regard, direction simulations of dynamical complex networks are necessary.

To this end, we employ the chaotic logistic map, $x_{t+1} = f(x_t) = ax_n(1 - x_n)$ with $a = 4$, as the node dynamics, and we set the coupling function as $H(x) = x$. For this logistic map, the synchronization constraint can be calculated analytically, which is $R_c = 3$. The uniform coupling strength is $\varepsilon = 1$. The initial network consists of six globally connected maps, with their initial states chosen randomly from the range $(0,1)$. After the network is synchronized, we start to grow it by subsequently introducing new nodes (of dynamics identical to the existing nodes) onto it. The new node is of random initial condition and is connected to six of the existing nodes in a random fashion. Whether the new node j is accepted by the network is judged by the synchronization error $\Delta(t) = \Sigma_{i,j=1}^{n}|x_j(t) - x_i(t)|/[n(n-1)]$, with $i = 1, \ldots, n$ the node index. After a transient period of 500 iterations, if $\Delta < 10^{-5}$, the enlarged network is regarded as synchronizable and the new node will be accepted. Otherwise, the new node will be rejected. The growing process continues until the network reaches the size $n = 600$. The degree distribution of the failed additions, $P(k_f)$, is plotted in Fig. 10(a). It is found that the distribution follows roughly a power-law scaling, with the fitted exponent at about -3.8.

The degree distribution, $P(k)$, of the generated network is plotted in Fig. 10(b). It is also found to follow a power-law scaling, with the fitted exponent at about -3.2. As a comparison, networks that are generated by the same set of network parameters but without the synchronization constraint are also analyzed. As depicted in Fig. 10(b), the difference between the degree distributions of the constrained and nonconstrained networks is distinct. These results are consistent with the eigenvalue analysis [Figs. 6(b) and Fig. 7], especially the power-law feature of the distributions.

In addition to the case of $a = 4$ of the logistic map, we have also checked numerically the growth of complex networks constituted by other local dynamics, including the chaotic logistic map with the parameter $a = 3.8$, and the chaotic Rössler oscillator [56]. The general observation is that, if the adiabatic condition $T_s \ll T_g$ is fulfilled and the synchronization constraint plays effect, the generated network always has a clear scale-free feature when the network size is large enough ($n > 500$). Additionally, the scale-free feature of the constrained network is also found to be robust to the noise perturbations. For instance, for the same network growth as that of Fig. 10, we have added independent and identically distributed (i.i.d.) random noise of amplitude 1×10^{-2} onto

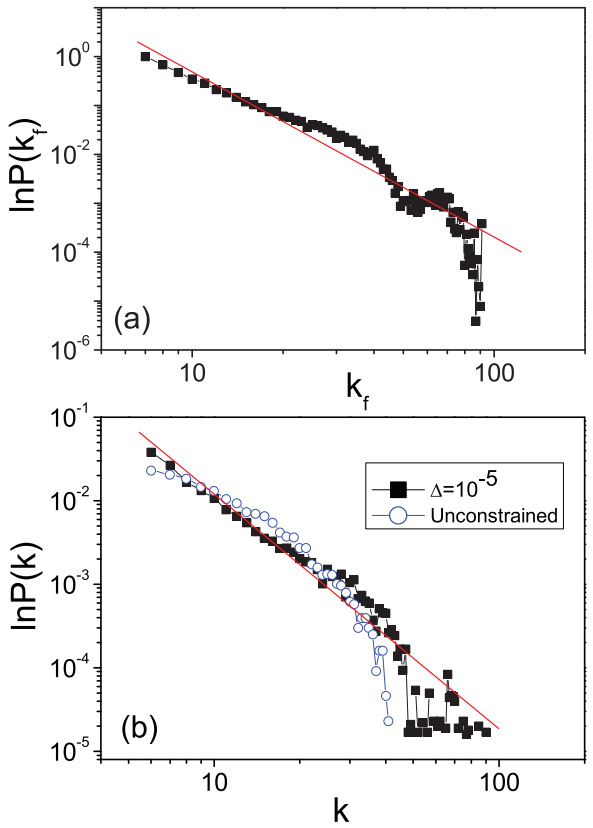

FIG. 10. (Color online) For a growing network of coupled chaotic logistic maps, (a) the degree distribution, $P(k_f)$, of the failed nodes, and (b) the degree distribution, $P(k)$, of the generated network of size $n = 600$. The fitted exponents in (a) and (b) are -3.8 and -3.2, respectively. As a comparison, the degree distribution of the network generated without the synchronization constraint is also plotted. Please see the text for a detailed description of the model. Each datum is averaged over 24 network realizations.

the dynamics of the network nodes, and we found that the network structure is almost the same as the noise-free case.

VI. DISCUSSIONS AND CONCLUSION

In network modeling, a key ingredient for generating networks of scale-free features is the link preferential attachment. Specifically, to have a power-law degree distribution, the probability for an existing node to be attached by the new link should be increasing *linearly* with its degree. If this linear relationship is not fulfilled, the scale-free feature of the network will be generally destroyed; e.g., the nonlinear preferential attachment $\Pi(k) \sim k^{\alpha}$ with $\alpha > 1$ or $\alpha < 1$ will lead to non-scale-free networks [57]. Noticing that in our model of a constrained random network, although the new node is attached to the network in a random fashion, the generated network is still of a clear scale-free feature. This makes it interesting to check whether the synchronization constraint—a new mechanism for node attachment—could provide "exactly" the same function as the preferential attachment. In other words, if we consider only the accepted nodes, we want to know from the numerical results whether they are attached to the network in the form of a linear preferential attachment.

In our simulations, we have focused mainly on two types of degree distributions: one for the failed nodes, $P(k_f)$, and the other for the generated network, $P(k)$. Assuming that after a transient process of network growth these distributions are stabilized onto some stable forms (this feature is observed in our simulations), then we have

$$P(k_f) = P(k)/\Pi'(k), \tag{6}$$

with $\Pi'(k)$ the attaching function induced by the synchronization constraint. The eigenvalue analysis of Figs. 6(b) and 7(a) shows that $P(k_a) \sim k^{-3.4}$ and $P(k) \sim k^{-2.7}$. From Eq. (6), we thus have $\Pi'(k) \sim k^{0.7}$. The direction simulations of Fig. 10 show that $P(k_a) \sim k^{-3.8}$ and $P(k) \sim k^{-3.2}$. We thus have $\Pi'(k) \sim k^{0.6}$. In both cases, the attachment is of the nonlinear form $\Pi'(k) \sim k^{\alpha}$, with $\alpha < 1$. As we discussed above, in the conventional model of a growing network, the nonlinear attachment will usually destroy the scale-free feature. However, our study suggests that, even with a nonlinear attachment, the generated network could still be possessing the scale-free feature.

The generation of a scale-free network without a linear preferential attachment might be due to the following reasons. One possibility could be the limited simulations. In our study, due to the heavy computation, the network growth is stopped at $n = 2 \times 10^3$ for eigenvalue analysis and $n = 600$ for direct simulations. At the current stage, it is not clear whether the obtained scalings, mainly the two degree distributions, still stand when the network size is large enough, e.g., $n > 5 \times 10^3$. If the scalings vary with the network size, then the above derivation of nonlinear attachment should be rechecked. Another possibility could be that the nonlinear attachment *indeed* could generate a scale-free network. This is possible because in our model of a constrained network, the attachment is *dynamically* varying with the network collective dynamics, which might provide a totally new mechanism for preferential attachment. We hope these questions can be addressed in future studies.

An important message delivered by the present study is that, besides the aspects of robustness and efficiency (small network diameter), a scale-free property is also a natural demand of the stability of network dynamics. This provides a solid base for the emergence of a scale-free feature in the evolution of dynamical complex systems, say, for example, neural networks [2]. Meanwhile, as a universal phenomenon in nature, the synchronization of networked nonlinear oscillators has important implications to the functionality of many realistic systems, ranging from biological to technological systems [58]. The present study also indicates that, as two typical phenomena of complex systems, the synchronization behavior and the scale-free property are closely related to each other.

In Ref. [7], a method for measuring the attaching form of realistic networks has been proposed. In this method, without the problem of node failures, the preferential attachment can be inferred from the degree of the attached nodes in a direct manner. We wish to note that this method is essentially the same as the analysis of failed additions, i.e., $P(k_f)$, used in the present paper, since the probability of successfully

attaching a link is inversely proportional to that of missing the link. Actually, this relationship has been used in Eq. (6). We also wish to note that, in characterizing the network structure, we have employed only the very basic topological properties, including the degree distribution, the average network diameter, and the clustering coefficient. Currently, it is still unknown whether the constrained network has some unique topological properties, e.g., the community structure, node assortativity, etc. [48], and how these properties are dependent on the synchronization constraint.

In summary, we have investigated the growth of a complex network under the constraint of network synchronization. Our studies show that, constrained by the synchronization stability, the network will grow in a selective and dynamical fashion. An interesting finding is that, with dynamical growth, the generated network presents the scale-free feature even without the linear form of preferential attachment. Our studies highlight the fact that, driven by the network collective dynamics, the evolution of the network structure could also consist of rich dynamics.

ACKNOWLEDGMENTS

This work was supported by the National Natural Science Foundation of China under Grant No. 10805038, and by the Chinese Universities Scientific Fund.

[1] R. Albert and A.-L. Barabási, Rev. Mod. Phys. **74**, 47 (2002).
[2] M. E. J. Newman, SIAM Rev. **45**, 167 (2002).
[3] S. N. Dorogovtsev and J. F. F. Mendes, Adv. Phys. **51**, 1079 (2002).
[4] A. L. Barabási and R. Albert, Science **286**, 509 (1999).
[5] M. Faloutsos, P. Faloutsos, and C. Faloutsos, Comput. Commun. Rev. **29**, 251 (1999).
[6] A. Broder, R. Kumar, F. Maghoul, P. Raghavan, S. Rajalopagan, R. Stata, A. Tomkins, and J. Wiener, Comput. Netw. **33**, 309 (2000).
[7] H. Jeong, Z. Néda, and A.-L. Barabási, Europhys. Lett. **61**, 567 (2003).
[8] M. E. J. Newman, Phys. Rev. E **64**, 025102(R) (2001).
[9] A. Vazquez, R. Pastor-Satorras, and A. Vespignani, Phys. Rev. E **65**, 066130 (2002).
[10] P. Crucitti, V. Latora, and M. Marchiori, Physica A **338**, 92 (2004).
[11] D. P. Chassin and C. Posse, Physica A **355**, 667 (2005).
[12] M. L. Sachtjen, B. A. Carreras, and V. E. Lynch, Phys. Rev. E **61**, 4877 (2000).
[13] P. Crucitti, V. Latora, and M. Marchiori, Phys. Rev. E **69**, 045104 (2004).
[14] P. Holme and B. J. Kim, Phys. Rev. E **65**, 066109 (2002).
[15] A. E. Motter and Y.-C. Lai, Phys. Rev. E **66**, 065102(R) (2002).
[16] R. M. May, Nature (London) **238**, 413 (1972).
[17] S. R. Proulx, D. E. L. Promislow, and P. C. Phillips, Trends Ecol. Evol. **20**, 345 (2005)
[18] J. I. Perotti, O. V. Billoni, F. A. Tamarit, D. R. Chialvo, and S. A. Cannas, Phys. Rev. Lett. **103**, 108701 (2009).
[19] P. Oikonomou and P. Cluzel, Nat. Phys. **2**, 532 (2006).
[20] F. C. Santos, J. M. Pacheco, and T. Lenaerts, Proc. Natl. Acad. Sci. U.S.A. **103**, 3490 (2006).
[21] D. Garlaschelli, A. Capocci, and G. Caldarelli, Nat. Phys. **3**, 813 (2007).
[22] L. Donetti, P. I. Hurtado, and M. A. Munoz, Phys. Rev. Lett. **95**, 188701 (2005).
[23] P. M. Gleiser and D. H. Zanette, Eur. Phys. J. B **53**, 233 (2006).
[24] A. E. Motter and Z. Toroczkai, Chaos **17**, 26101 (2007).
[25] M. Brede, Eur. Phys. J. B **62**, 87 (2008).
[26] P. A. Robinson, J. A. Henderson, E. Matar, P. Riley, and R. T. Gray, Phys. Rev. Lett. **103**, 108104 (2009).
[27] A. Arenas, A. Diaz-Guilera, J. Kurths, Y. Moreno, and C. Zhou, Phys. Rep. **469**, 93 (2008).
[28] P. Gong and C. V. Leeuwen, Europhys. Lett. **67**, 328 (2004).
[29] R. K. Pan and S. Sinha, Phys. Rev. E **76**, 045103(R) (2007).
[30] T. S. Evans and A. D. K. Plato, Phys. Rev. E **75**, 056101 (2007).
[31] F. Sorrentino and E. Ott, Phys. Rev. Lett. **100**, 114101 (2008).
[32] D. J. Watts and S. H. Strogatz, Nature (London) **393**, 440 (1998).
[33] X. F. Wang and G. Chen, Int. J. Bifurcation Chaos Appl. Sci. Eng. **12**, 187 (2002).
[34] T. Nishikawa, A. E. Motter, Y.-C. Lai, and F. C. Hoppensteadt, Phys. Rev. Lett. **91**, 014101 (2003).
[35] A. E. Motter, C. S. Zhou, and J. Kurths, Europhys. Lett. **69**, 334 (2005).
[36] X. G. Wang, Y.-C. Lai, and C. H. Lai, Phys. Rev. E **75**, 056205 (2007).
[37] C. T. Butts, Science **325**, 414 (2009).
[38] D. Drachman, Neurology **64**, 2004 (2005).
[39] L. M. Pecora and T. L. Carroll, Phys. Rev. Lett. **80**, 2109 (1998).
[40] G. Hu, J. Z. Yang, and W. Liu, Phys. Rev. E **58**, 4440 (1998).
[41] M. Barahona and L. M. Pecora, Phys. Rev. Lett. **89**, 054101 (2002).
[42] L. Huang, Q. Chen, Y.-C. Lai, and L. M. Pecora, Phys. Rev. E **80**, 036204 (2009).
[43] F. Chung, L. Lu, and V. Vu, Proc. Natl. Acad. Sci. U.S.A. **100**, 6313 (2003).
[44] A. E. Motter, C. Zhou, and J. Kurths, Phys. Rev. E **71**, 016116 (2005).
[45] A.-L. Barabási, R. Albert, and H. Jeong, Physica A **272**, 173 (1999).
[46] [http://moat.nlanr.net/AS/Data/ASconnlist.20000102.946809601].
[47] R. Albert, H. Jeong, and A. L. Barabási, Nature (London) **406**, 378 (2000).
[48] L. D. Costa, F. A. Rodrigues, G. Travieso, and P. R. V. Boas, Adv. Phys. **56**, 167 (2007).
[49] H. Jeong, B. Tombor, R. Albert, Z. N. Oltvai, and A.-L. Barabási, Nature (London) **407**, 651 (2000).
[50] J. M. Montoya and R. V. Solé, e-print arXiv:cond-mat/0011195.
[51] M. J. Keeling, Proc. R. Soc. London, Ser. B **266**, 859 (1999).

[52] P. L. Krapivsky and S. Redner, Phys. Rev. E **63**, 066123 (2001).
[53] P. N. McGraw and M. Menzinger, Phys. Rev. E **77**, 031102 (2008).
[54] M. Timme, T. Geisel, and F. Wolf, Chaos **16**, 015108 (2006).
[55] S.-W. Son, H. Jeong, and H. Hong, Phys. Rev. E **78**, 016106 (2008).
[56] O. E. Rössler, Phys. Lett. **57A**, 397 (1976).
[57] P. L. Krapivsky, S. Redner, and F. Leyvraz, Phys. Rev. Lett. **85**, 4629 (2000).
[58] A. S. Pikovsky, M. G. Rosenblum, and J. Kurths, *Synchronization: A Universal Concept in Nonlinear Science* (Cambridge University Press, Cambridge, UK, 2001).